



Entangled zinc–ditetrazolate frameworks involving in situ ligand synthesis and topological modulation by various secondary N-donor ligands

Yun-Wu Li, Wei-Lin Chen, Yong-Hui Wang*, Yang-Guang Li, En-Bo Wang*

Key Laboratory of Polyoxometalate Science of Ministry of Education, Department of Chemistry, Northeast Normal University, Renmin Street No. 5268, Changchun, Jilin 130024, PR China

ARTICLE INFO

Article history:

Received 14 October 2008

Received in revised form

17 December 2008

Accepted 29 December 2008

Available online 7 January 2009

ABSTRACT

The introduction of various secondary N-donor ligands into an in situ ditetrazolate–ligand synthesis system of terephthalonitrile, NaN_3 and ZnCl_2 led to the formation of three new entangled frameworks $\text{Zn}(\text{pdtz})(4,4'\text{-bipy}) \cdot 3\text{H}_2\text{O}$ (**1**), $[\text{Zn}(\text{pdtz})(\text{bpp})]_2 \cdot 3\text{H}_2\text{O}$ (**2**) and $\text{Zn}(\text{pdtz})_{0.5}(\text{N}_3)(2,2'\text{-bipy})$ (**3**) (4,4'-bipy = 4,4'-bipyridine; bpp = 1,3-bis(4-pyridyl)propane; 2,2'-bipy = 2,2'-bipyridine; H_2pdtz = 5,5'-1,4-phenylene-ditetrazole). The formation of pdtz^{2-} ligand involves the Sharpless [2+3] cycloaddition reaction between terephthalonitrile and NaN_3 in the presence of Zn^{2+} ion as a Lewis-acid catalyst under hydrothermal conditions. Compound **1** exhibits a fivefold interpenetrating 3D framework based on the diamondoid topology. Compound **2** displays a twofold parallel interpenetrating framework based on the wavelike individual network. Compound **3** possesses a 2D puckered network. These new Zn–ditetrazolate frameworks are highly dependent on the modulation of different secondary N-donor ligands. Their luminescent properties were investigated.

© 2009 Elsevier Inc. All rights reserved.

1. Introduction

The design and synthesis of entangled metal–organic frameworks have recently witnessed explosive growth in the areas of inorganic chemistry, coordination chemistry, crystal engineering and materials science, not only due to their intrinsic aesthetics value but also their potential applications in catalysis, gas storage, molecular adsorption, optical, electronic and magnetic materials [1–49]. Although it is still difficult to prepare fully predictable entangled structures based on the rational design, recent rapid developments in coordination and organic chemistry provide more and more knowledge and possibilities for the creative synthesis of desired entangled frameworks [29–37]. Especially in recent years, entangled frameworks have been well developed and systematically discussed in comprehensive reviews by Batten, Robson and Carlucci. In general, the entangled frameworks should possess at least two important structural factors: one is that their independent chain-, layer- or framework-units should contain meshes or pores which are large enough for interpenetration. The other, which is necessary, is that these individual building units should possess the undulating structural feature [1–23]. Undoubtedly, various long chain-like N-donor ligands with diverse flexibility such as bipyridine- and biimidazole-containing

ligands are good candidates for the assembly of versatile entangled structures, mainly because of their propensity to form large voids or corrugation [20–49]. At this point, the bitetrazolate-containing ligands are also one kind of suitable building blocks since the tetra-N-donor property of the tetrazolate group can provide more coordination sites for metal centers to form complicated frameworks. Generally, the tetrazolate-containing ligands can be obtained from the classical Sharpless [2+3] cycloaddition reactions between cyano precursor and azide group, following by a series of complicated separation and purification steps [50]. A recent advance in this synthesis suggests a shortcut, that is, the in situ synthesis of the tetrazolate-containing ligands from the cyano and azide precursors in a hydrothermal environment with various transition metal ions as the Lewis acid catalysts (as shown in Scheme S1) [51–70]. Recently, Xiong et al. have reported a series of metal–monotetrazolate-based compounds isolated from such an in situ ligand synthesis system [57–61,66–70]. Obviously, this method also suggests a possible route for the exploration of entangled metal–ditetrazolate systems. However, such reaction systems based on in situ synthesis of ditetrazolate ligands has been far unexplored [62–70]. A possible reason is that these metal–ditetrazolate systems have few controllable factors to create, modulate or change the structural topologies during the assembly process. Nevertheless, the use of auxiliary ligands with various flexibility and coordination modes has proved to be an efficient way to dramatically influence the structural topologies [29–37,66–70]. Therefore, utilizing secondary ligands in the above reaction

* Corresponding authors. Fax: +86 431 85098787.

E-mail addresses: wangyh319@nenu.edu.cn (Y.-H. Wang), wangenbo@public.cc.jl.cn, Wangenb889@nenu.edu.cn (E.-B. Wang).

systems may provide a promising strategy for the construction of new entangled metal–dinitrazolate frameworks.

Based on the aforementioned considerations, we deliberately chose an in situ synthesis system of 5,5'-1,4-phenylene-ditrazole (H_2pdtz) ligands via mixing terephthalonitrile, NaN_3 and ZnCl_2 (acting as Lewis acid catalyst), assisted with various secondary N-donor ligands such as 4,4'-bipyridine (4,4'-bipy), 1,3-bis(4-pyridyl)propane (bpp) and 2,2'-bipyridine (2,2'-bipy). Our aim was to explore new entangled Zn–dinitrazolate frameworks and investigate the effect of various auxiliary ligands on the ultimate frameworks. Herein, we report three Zn–dinitrazolate-based compounds, $\text{Zn}(\text{pdtz})(4,4'\text{-bipy}) \cdot 3\text{H}_2\text{O}$ (**1**), $[\text{Zn}(\text{pdtz})(\text{bpp})]_2 \cdot 3\text{H}_2\text{O}$ (**2**) and $\text{Zn}(\text{pdtz})_{0.5}(\text{N}_3)(2,2'\text{-bipy})$ (**3**). Compounds **1** and **2** exhibit different interpenetrating frameworks, while compound **3** possesses undulated networks. Their structural topologies are highly dependent on the secondary N-donor ligands. The crystal structures, topological analyses and luminescent properties of **1–3** have been well investigated.

2. Experimental section

2.1. Materials and methods

All chemicals purchased were of reagent grade and used without further purification. Elemental analyses (C, N, and H) were performed on a Perkin–Elmer 2400 CHN elemental analyzer. FT/IR spectra were recorded in the range 4000–400 cm^{-1} on an Alpha Centaur FT/IR spectrophotometer using KBr pellets. TG analyses were performed on a Perkin–Elmer TGA7 instrument in flowing N_2 with a heating rate of 10 $^\circ\text{C min}^{-1}$. Photoluminescence spectra were measured at room temperature using a FL-2T2 instrument (SPEX, USA) with a 450-W xenon lamp monochromatized by double gratings (1200 g mu^{-1}).

Caution! Azide salts are potentially explosive and should be handled in small quantities and with adequate precautions.

2.2. Synthesis of compounds 1–3

2.2.1. Synthesis of $\text{Zn}(\text{pdtz})(4,4'\text{-bipy}) \cdot 3\text{H}_2\text{O}$ (**1**)

Compound **1** was synthesized from a mixture of ZnCl_2 (0.068 g, 0.5 mmol), NaN_3 (0.039 g, 0.6 mmol), terephthalonitrile (TPN) (0.038 g, 0.3 mmol), 4,4'-bipy (0.047 g, 0.3 mmol), NaOH (0.01 g,

0.25 mmol) and H_2O (10 mL). This mixture was stirred for 20 min at room temperature. Then the above mixture was transferred into a Teflon-lined autoclave (20 mL) and kept at 120 $^\circ\text{C}$ for 3 days. After the reaction mixture had been slowly cooled at a rate of 10 $^\circ\text{C h}^{-1}$ to room temperature, block-like colorless crystals of **1** were obtained. The products were collected by filtration, washed with distilled water and dried in a desiccator at room temperature (yield: 58% based on Zn). Elemental analysis for $\text{C}_{18}\text{H}_{18}\text{N}_{10}\text{O}_3\text{Zn}$ ($M_r = 487.81$) (**1**): calcd: C 44.32, H 3.72, N 28.71%; found: C 44.28, H 3.69, N 28.72%. Selected IR data (KBr pellet, cm^{-1}): 3348 (br), 1671 (m), 1612 (s), 1556 (m), 1535 (m), 1429 (s), 1272 (w), 1232 (m), 1170 (m), 1141 (m), 1071 (m), 1044 (m), 1009 (m), 865 (m), 817 (s), 751 (m), 727 (m), 647 (m), 545 (w), 491 (m), 460 (m).

2.2.2. Synthesis of $[\text{Zn}(\text{pdtz})(\text{bpp})]_2 \cdot 3\text{H}_2\text{O}$ (**2**)

Compound **2** was prepared with a similar procedure to **1** except that 4,4'-bipy was substituted by bpp (0.059 g, 0.3 mmol). Block-like colorless crystals of **2** were obtained (yield: 62% based on the Zn). Elemental analysis for $\text{C}_{42}\text{H}_{42}\text{N}_{20}\text{O}_3\text{Zn}_2$ ($M_r = 1005.70$) (**2**): calcd: C 50.16, H 4.21, N 27.85%; found: C 50.13, H 4.18, N 27.88%. Selected IR data (KBr pellet, cm^{-1}): 3423 (br), 2075 (m), 1622 (s), 1558 (m), 1510 (w), 1437 (s), 1342 (w), 1229 (m), 1163 (m), 1141 (w), 1068 (m), 1038 (m), 1006 (m), 862 (m), 805 (m), 752 (m), 623 (w), 527 (w), 489 (m).

2.2.3. Synthesis of $\text{Zn}(\text{pdtz})_{0.5}(\text{N}_3)(2,2'\text{-bipy})$ (**3**)

Compound **3** was synthesized in an analogous manner to **1** except that 4,4'-bipy was replaced by 2,2'-bipy (0.047 g, 0.3 mmol) and a little more NaN_3 (0.046 g, 0.7 mmol) was used during the preparation. Block-like colorless crystals of **3** were isolated (yield: 48% based on the Zn). Elemental analysis for $\text{C}_{14}\text{H}_{10}\text{N}_9\text{Zn}$ ($M_r = 369.68$) (**3**): calcd: C 45.49, H 2.73, N 34.10%; found: C 45.45, H 2.68, N 34.13%. Selected IR data (KBr pellet, cm^{-1}): 2049 (s), 1597 (m), 1565 (m), 1492 (m), 1433 (s), 1336 (m), 1319 (m), 1288 (m), 1252 (w), 1181 (m), 1155 (w), 1055 (w), 1020 (m), 902 (w), 890 (m), 770 (s), 734 (m), 651 (m), 629 (w), 540 (w), 493 (m), 420 (m).

2.3. X-ray crystallography

Crystallographic data for compounds **1–3** were collected at 150 K with a Rigaku R-axis Rapid IP diffractometer using graphite monochromatic $\text{MoK}\alpha$ radiation ($\lambda = 0.71073 \text{ \AA}$) and IP technique.

Table 1

Crystal data and structure refinement for **1–3**.

	1	2	3
Empirical formula	$\text{C}_{18}\text{H}_{18}\text{N}_{10}\text{O}_3\text{Zn}$	$\text{C}_{42}\text{H}_{42}\text{N}_{20}\text{O}_3\text{Zn}_2$	$\text{C}_{14}\text{H}_{10}\text{N}_9\text{Zn}$
Formula weight	487.79	1005.70	369.68
Crystal system	Monoclinic	Monoclinic	Monoclinic
Space group	$P2(1)/c$	$P2(1)/c$	$P2(1)/c$
<i>a</i> (Å)	6.7186(13)	12.876(3)	20.331(4)
<i>b</i> (Å)	17.082(3)	17.626(4)	10.608(2)
<i>c</i> (Å)	17.352(4)	10.479(2)	6.7771(14)
β ($^\circ$)	98.77(3)	101.57(3)	94.05(3)
Volume (Å ³)	1968.1(7)	2329.9(8)	1457.9(5)
Z	4	2	4
Calculated density (Mg m^{-3})	1.646	1.434	1.684
Absorption coefficient (mm^{-1})	1.295	1.092	1.702
<i>F</i> (000)	1000	1036	748
<i>R</i> (int)	0.0370	0.1273	0.0338
Goodness-of-fit on <i>F</i> ²	1.038	1.026	1.057
Final <i>R</i> ^a indices [$I > 2\sigma(I)$] (all data)	0.0308	0.0785	0.0349
<i>wR</i> ₂ ^b (all data)	0.0748	0.2123	0.0908

^a $R_1 = \sum ||F_o| - |F_c|| / \sum |F_o|$.

^b $wR_2 = [\sum (w(F_o^2 - F_c^2)^2) / \sum (w(F_o^2)^2)]^{1/2}$.

The structures were solved by the direct method and refined by the full-matrix least-squares method on F^2 using the SHELXTL 97 crystallographic software package [71,72]. All non-hydrogen atoms in the crystal data of **1–3** were refined anisotropically except the solvent water molecules in **2**. H atoms on their parent C atoms were fixed in geometrically calculated positions, while H atoms on water molecules in the crystal structure of **1** were determined from the difference Fourier maps. Further details of the X-ray structural analysis are given in Table 1. Selected bond lengths and angles of **1–3** are listed in Tables S1–S3, respectively.

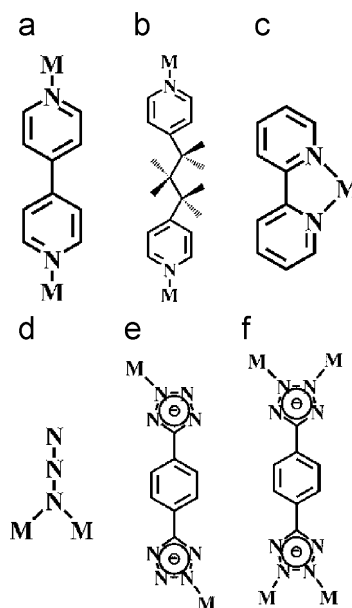
3. Results and discussion

3.1. Synthesis

Compounds **1–3** were hydrothermally synthesized from the in situ ditetrazolate-ligand synthesis system assisted with various secondary N-donor ligands. The ditetrazolate ligand pdtz^{2-} was in situ synthesized through the Sharpless [2+3] cycloaddition reaction between terephthalonitrile and azide in the presence of Zn^{2+} ion as the Lewis acid catalyst under hydrothermal reaction conditions (see Scheme 1) [51–56]. This in situ ligand synthesis is proved to be convenient and environmentally friendly. In contrast, the traditional synthetic method of tetrazolates in acidic media usually release a large amount of heat as well as hydrazoic acid and thus the whole reaction system becomes highly toxic and explosive [50]. During the present hydrothermal synthesis, various secondary N-donor ligands (4,4'-bipy, bpp and 2,2'-bipy) with different flexibility and coordination modes were introduced into the Zn-ditetrazolate system in order to modulate the structural topologies. As shown in Scheme 1, the use of rigid bridging-ligand 4,4'-bipy led to the isolation of compound **1**, which exhibits a fivefold interpenetrated 3D framework based on a diamondoid topology. In **1**, both 4,4'-bipy and pdtz^{2-} are rigid linear ligands, resulting in an individual framework with very large pores for further interpenetration (see Fig. S1). When the flexible bpp ligand was employed as the auxiliary ligand, compound **2** was isolated and displays a twofold parallel interpenetrating framework based on undulated layers. Although the Zn^{2+} ions in **2** exhibit a similar coordination mode to **1**, the bpp ligand endows itself an undulated TT (trans–trans) conformation (see Scheme 2(b)) [49], looking like the letter “M”, which partly inhibits the formation of large channels and thus decreases the possibility of multiple interpenetration. The successful preparation of **1** and **2** prompted us to try other auxiliary N-donor ligands. 2,2'-bipy, as one typical chelate ligand, usually plays important roles in “cutting” or “clipping” high-dimensional frameworks by occupying parts of the coordination sites on metal centers (Scheme 2(c)) and inducing low-dimensional wavelike networks or chains. The introduction of 2,2'-bipy into this Zn-ditetrazolate system led to the isolation of a puckered 2D networks of compound **3**. Such 2D layers also possess narrow pores, whereas the adjacent layers cannot interpenetrate with each other because



Scheme 1. Schematic view of the in situ pdtz -ligand synthesis system and the topological modulation by various N-donor ligands for compounds **1–3**.



Scheme 2. Coordination modes of ligands used in this article: (a) 4,4'-bipyridine; (b) 1,3-bis(4-pyridyl)propane (trans–trans conformation, TT); (c) 2,2'-bipyridine; (d) N_3^- (end-on); (e) and (f) 5,5'-1,4-phenylene-ditetrazole.

of the relative small meshes in the layers and the large steric hindrance from 2,2'-bipy ligands. It is worth mentioning that a little more azide ligand was used by accident during the synthesis of compound **3**, which has been subsequently proved a very important step to isolate the final compound because the azide ligand also acted as linkers to connect the Zn^{2+} ions in compound **3**. Furthermore, 2,2'-bipy plays a ‘passivating’ role in providing steric constraints which can prevent large pdtz^{2-} ligands from coordinating to the metal centers. If the same amount of azide was used as in the preparation of compound **1**, compound **3** could not be isolated.

In addition, a series of parallel experiments demonstrated that some factors such as the pH value, reaction temperature, the molar ratio and the concentration of the initial reagents were important to the isolation of the final crystalline products. Compounds **1–3** can only be prepared in a limited pH range (7.8–8.2), whereas no products can be obtained out of this pH range. If the pH value is lower than 7.8, the N_3^- groups may be hydrolyzed and release hydrazoic acid. At pH values higher than 8.2, the cyano groups are inclined to hydrolysis and form the carboxylate groups. In these syntheses, the pH value of the reaction system may be adjusted by the NaOH solution. On the other hand, it has been found that the above reactions can be carried out in the temperature range of $120 \pm 10^\circ\text{C}$. If the reaction temperature is much lower or higher than 120°C , no crystals can be obtained. It is also notable that changing the ratio or concentration of reagents does not result in the final compounds **1–3**.

3.2. Crystal structure of compounds **1–3**

3.2.1. Structure of $\text{Zn}(\text{pdtz})(4,4'\text{-bipy}) \cdot 3\text{H}_2\text{O}$ (**1**)

Single-crystal X-ray diffraction analysis reveals that compound **1** crystallizes in the monoclinic space group $P2_1/c$ and exhibits an interesting fivefold interpenetrated 3D framework based on a diamondoid topology. In the asymmetric unit of **1**, there is one Zn center, one pdtz^{2-} ligand, one 4,4'-bipy ligand and three solvent water molecules. As shown in Fig. S2, the Zn center exhibits a tetra-coordinated environment with two nitrogen atoms deriving

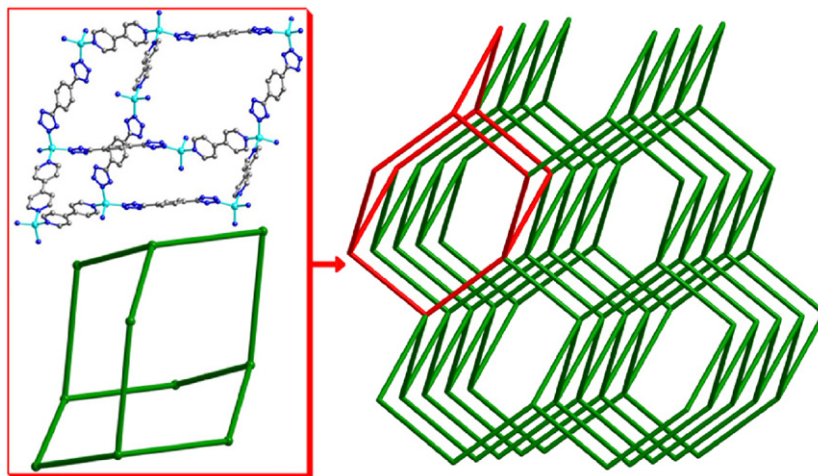


Fig. 1. Ball-and-stick view of the diamondoid cage unit (top-left) in **1**, its topological scheme (down-left) and individual diamond-type 3D topology (right).

from two different pdtz^{2-} ligands and two nitrogen atoms originating from two different 4,4'-bipy ligands. The bond lengths of Zn–N are in the range of 1.9713(19)–2.0253(19) Å and the bond angles of N–Zn–N vary from 108.66(8)° to 111.70(8)°. All pdtz^{2-} ligands possess the same diagonal bidentate coordination mode (μ -2,2'), that is, two N-donors from two tetrazolate groups coordinate with two different Zn atoms in a side-trans bridging fashion (see Scheme 2(e)). As a result, 10 Zn centers are connected by twelve bridging ligands, namely, six pdtz^{2-} and six 4,4'-bipy, generating a diamondoid cage (Fig. 1, left). Based on the secondary building unit (SBU) concept [24–28], tetrahedral $\{\text{ZnN}_4\}$ can be viewed as a tetrahedral SBU (Fig. S3, left), and the independent 3D diamondoid framework of **1** is composed of the tetrahedral SBUs connected by the linear linkers of pdtz^{2-} and 4,4'-bipy (Fig. 1 and S1). The topological analysis of **1** reveals that such a typical diamondoid framework contains large diamondoid cages with the topology symbol (6^6) [3,4,16,17,42,77] and exhibits cyclohexane-like windows in a chair conformation (Fig. 1 and S1) [73]. The distances between adjacent Zn...Zn centers linked by pdtz^{2-} and 4,4'-bipy bridges are 13.4055 and 11.1463 Å, respectively. The void space in an individual framework is so large that five identical 3D diamondoid frameworks can interpenetrate with each other to form a fascinating five-fold interpenetrating fashion along *b* axis (see Fig. 2). Such an interpenetration mode can minimize the big void cavities of the diamondoid cages. It is worth mentioning that such an interpenetration mode is the first example in the metal–triazolate system. Furthermore, the adjacent entangled diamondoid frameworks possess weak π - π interactions [74] between aromatic rings of neighboring pdtz^{2-} and 4,4'-bipy ligands. The centroid–centroid distances of the aromatic rings between parallel pdtz – pdtz and bipy – bipy are 3.942 and 4.091 Å, respectively. The isolated water molecules reside in the interspaces of the neutral channels.

3.2.2. Structure of $[\text{Zn}(\text{pdtz})(\text{bpp})]_2 \cdot 3\text{H}_2\text{O}$ (**2**)

Single-crystal X-ray diffraction analysis shows that compound **2** also crystallizes in the monoclinic space group $P2_1/c$ but displays a twofold parallel interpenetration framework based on undulated layers. In the asymmetric unit of **2**, there is one crystallographically unique Zn center, one pdtz^{2-} ligand, one bpp ligand and three solvent water molecules (as shown in Fig. S4). All the Zn centers exhibit the $\{\text{ZnN}_4\}$ tetrahedral coordination geometry with two N atoms derived from two different pdtz^{2-} ligands and the other two N atoms from different bpp ligands. The bond

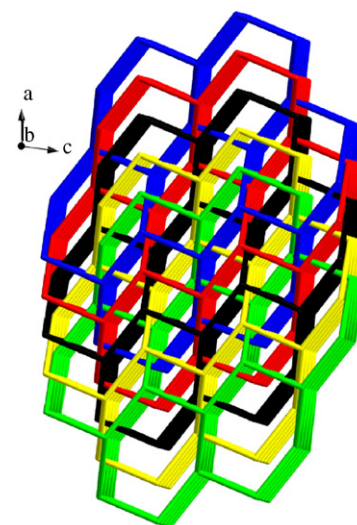


Fig. 2. Fivefold interpenetrating 3D framework of **1** based on the (6^6)-diamondoid topology.

lengths of Zn–N are in the range of 1.963(6)–2.022(5) Å and the bond angles of N–Zn–N vary from 102.8(2)° to 115.2(2)°. Both bpp ligands possess the undulated TT conformation [49,75], looking like the letter “M”. The distance between two N-donors is 9.6 Å (see Scheme 2(b)). All pdtz^{2-} ligands adopt the same coordination modes as those in compound **1**. Based on above coordination modes, all the Zn centers are linked by the pdtz^{2-} and bpp ligands into a 2D wavelike network with square meshes (see Fig. 3) and the topology symbol of the layer should be (4·4) [73]. The square size is ca. 12.9 Å × 13.2 Å (see Fig. S5). Such an undulated sheet with large square pores offers an ideal condition for the interpenetration. Actually, two identical sets of 2D parallel layers in **2** are interlocked with each other to form a two-fold parallel interpenetration framework (see Fig. 4). Furthermore, all solvent water molecules in **2** reside in the interspaces of the polycatenation framework. However, no visible channels can be found from the 3D packing arrangements (see Fig. S6), indicating that the crystal structure of **2** contains relatively small and close interspaces. In addition, the π - π interactions between the aromatic rings of pdtz^{2-} and bpp ligands may further stabilize the whole 3D framework.

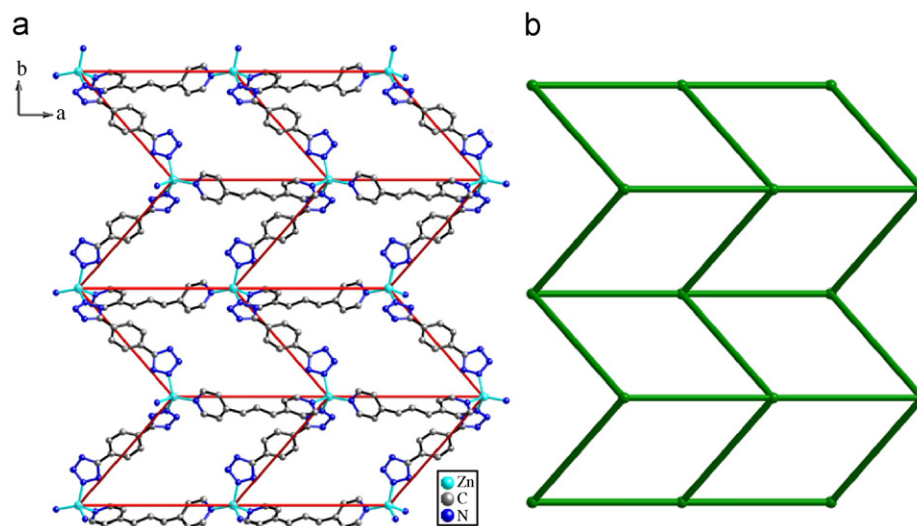


Fig. 3. (a) Ball-and-stick view of the individual 2D undulated network with (4×4) -topology in **2**; (b) Topological scheme of the 2D undulated network in **2**.

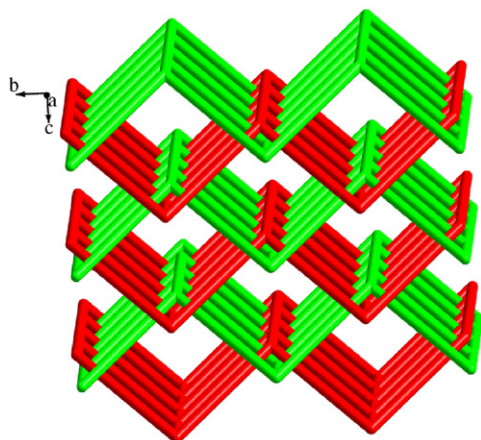


Fig. 4. Schematic representation of the twofold "parallel" interpenetration architecture of **2** along *a* axis.

3.2.3. Structure of $\text{Zn}(\text{pdtz})_{0.5}(\text{N}_3)(2,2'\text{-bipy})$ (**3**)

When linear ligands 4,4'-bipy or bpp are replaced by the chelate ligand 2,2'-bipy, compound **3** is obtained. Single-crystal X-ray diffraction analysis shows that compound **3** crystallizes in the monoclinic space group $P2_1/c$ and exhibits a 2D puckered network. In the asymmetric unit of **3**, there is one Zn center, half the pdtz^{2-} ligand, one azido ligand, and one 2,2'-bipy ligand (as shown in Fig. S7). Different from the tetrahedral coordination geometry of $\{\text{ZnN}_4\}$ in compounds **1** and **2**, the Zn centers in **3** possess a distorted $\{\text{ZnN}_6\}$ octahedral coordination geometry with two N atoms deriving from two different pdtz^{2-} ligands, two from one chelate 2,2'-bipy ligand, and the last two from two azido groups. The pdtz^{2-} ligands also exhibit different coordination fashions in contrast to those in compounds **1** and **2**. In this case, the pdtz^{2-} ligands act as a quadridentate ligand (namely μ -2,3:2',3') coordinating with four Zn centers (see Scheme 2(f)). The 2,2'-bipy serves as a chelate ligand occupying two coordination sites of the Zn centers. Interestingly, the azide ligands also enter into the framework and act as linkers in an end-on (EO) mode to connect two adjacent Zn centers (see Scheme 2(d)). The bond distances between Zn and N-donor of azide ligands are in the range of 2.128(3)–2.491(3) Å, while the Zn–N_(azide)–Zn angle is 114.91(11)°. All the other bond lengths of Zn–N in **3** are in the

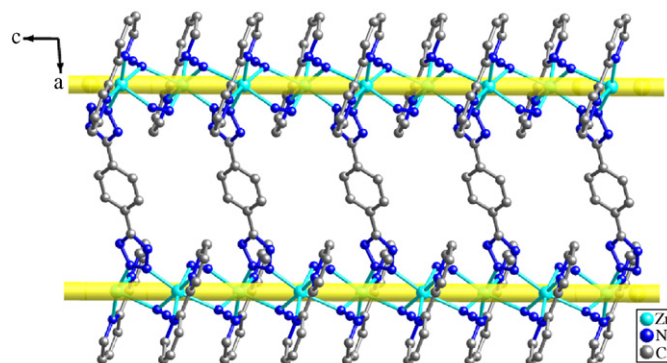


Fig. 5. Ball-and-stick view of the 1D chain in **3** based on Zn^{2+} , N_3^- and tetrazolate groups along the *c*-direction.

range of 2.086(2)–2.180(2) Å, and the bond angles of N–Zn–N vary from 75.98(7)° to 168.29(9)°. It is noteworthy that compound **3** represents the first metal–tetrazolate compound assisted with two types of auxiliary ligands at the same time. Based on above coordination modes, all the Zn centers are bridged by azide and tetrazolate group of pdtz^{2-} ligands into a 1D chain running along the *c*-direction (Fig. 5). These 1D chains are further connected by the pdtz^{2-} ligands into a 2D puckered layer (Fig. 5, 6(a)). In such a network, the intra-chain Zn...Zn distance is 3.899(1) Å and inter-chain ones are 13.022(6) and 10.608(2) Å, respectively (see Fig. 6(a)). Furthermore, these 1D chains are decorated by 2,2'-bipy ligands on both sides of the undulated layer (see Fig. 6(a)). Because of such obvious steric hindrance of the 2,2'-bipy ligands on the layers, no interpenetration can be realized between the adjacent puckered networks. From the topological point of view (as shown in Scheme S2), the pdtz^{2-} ligand can be abstracted as a flat ribbon, while the building unit $\{\text{Zn}_2\text{N}_3\}$ can be rationalized as a solid rod [76]. Since 2,2'-bipy ligands only act as a decorating ligand, it is not necessary to consider it in the topological analysis. Based on this simplification, the networks of **3** can be abstracted into a 2D undulated layer (Fig. 6(b), S8).

3.3. IR spectrum

In the IR spectra of compounds **1**, **2** and **3** (Fig. S9), the diagnostic peak of the cyano group at 2100 cm^{-1} disappeared,

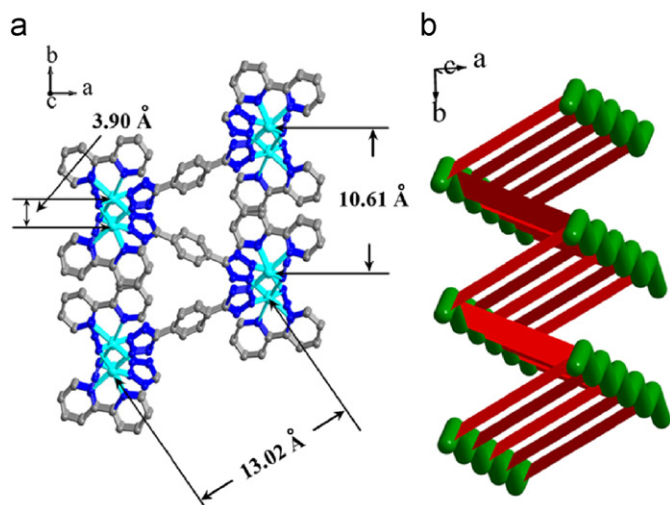


Fig. 6. (a) Ball-and-stick representation of the 2D puckered network in **3** viewed along *c* axis; (b) Topological scheme of the 2D sheet in **3** along *c* axis.

however, the emergence of the characteristic peaks (at 1612, 1556, 1535 and 1429 cm^{-1} for **1**, at ca. 1622, 1558, 1510 and 1437 cm^{-1} for **2**, and at ca. 1597, 1565, 1475 and 1433 cm^{-1} for **3**) suggests the formation of tetrazolate groups, in good agreement with those of tetrazolate-based compounds previously reported [57–70]. The existence of the bridging azide groups in the final framework of **3** is confirmed by the appearance of a strong band at 2049 cm^{-1} in the IR spectrum, which is attributed to the typical asymmetric stretching of N_3^- . Furthermore, the $\nu_s(\text{N}_3^-)$ stretching bands located at 1319 and 1288 cm^{-1} indicate that the N_3^- should be in an EO bridging mode [77–80]. In addition, the fingerprint peaks of 4,4'-bipy, bpp and 2,2'-bipy are overlapped with those of bptz^{2-} in lower wavenumber regions and can not be exactly assigned. Peaks at 3348 and 3423 cm^{-1} in the IR of compounds **1** and **2** are attributed to the vibration of water molecules, respectively. All the peak assignments are in agreement with the results of the single-crystal X-ray diffraction studies.

3.4. Thermal analysis

The TG curves of compounds **1** and **2** (see Fig. S10(a) and (b)) both exhibit two weight-loss steps. The first minor weight-loss of 11.48% of **1** ranging from 106 to 162 $^{\circ}\text{C}$ (5.42% of **2** between 108 and 136 $^{\circ}\text{C}$) corresponds to the release of the lattice water molecules. The second weight-loss of 75.06% of **1** in the temperature range of 196–450 $^{\circ}\text{C}$ (81.62% of **2** between 182 and 380 $^{\circ}\text{C}$) can be ascribed to the loss of all organic ligands. The whole weight losses of 86.54% (for **1**) and 87.05% (for **2**) are in good agreement with the calculated values 86.59% (**1**) and 86.99% (**2**), respectively. The TG curve of compound **3** exhibits a different weight-loss feature (as shown in Fig. S10(c)). Only one continuous weight-loss step was found in the temperature range of 228–376 $^{\circ}\text{C}$ with the whole weight loss of 82.14%, attributed to the successive release of ptz^{2-} , N_3^- and 2,2'-bipy ligands. This result is also well consistent with the calculated value 82.31%.

3.5. Fluorescent properties

The luminescent properties of compounds **1**, **2** and **3** were investigated in the solid state at room temperature. Since complexes **1**, **2**, and **3** are stable in air and insoluble in water or most organic solvents, no additional measurements in solution

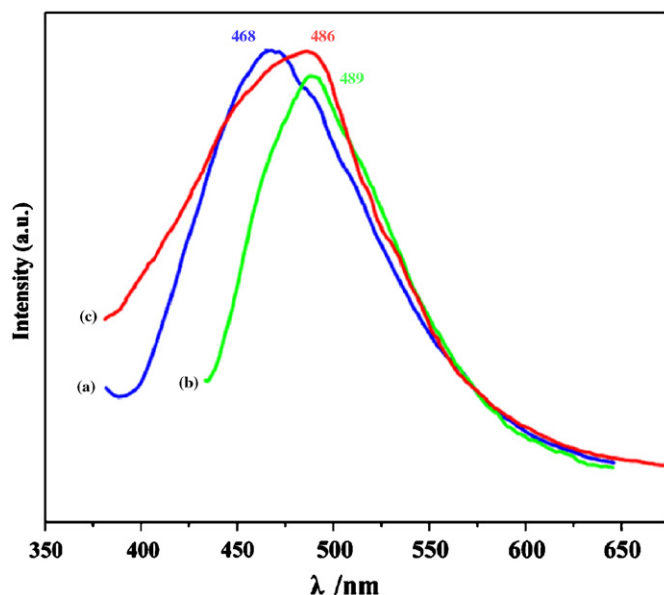


Fig. 7. Solid-state emission spectra of (a) **1** (excited at 358 nm), (b) **2** (excited at 410 nm) and (c) **3** (excited at 416 nm).

were performed. As shown in Fig. 7, **1**, **2** and **3** all exhibit strong fluorescent emission with the maxima at 468, 489 and 486 nm upon excitation at 358, 410 and 416 nm, respectively. This observation suggests that all three compounds may be excellent candidates for potential blue-emitted photoactive materials. In order to understand the nature of these emission bands, we compared the emission spectra of the three compounds and those of free organic ligands. The free H_2ptz ligand usually displays a broad emission peak with the emission maximum located at 473 nm [65], while the free 4,4'-bipy ligand does not emit any luminescence in the range of 400–800 nm [81,82]. As shown in Fig. 7, compound **1** exhibits a similar emission peak at 468 nm to the free H_2ptz ligand. Hence, the emission of **1** can be tentatively attributed to the intraligand transition of the Zn-modified ptz^{2-} ligands. In addition, the free bpp ligand usually emits intense luminescence at ca. 523 nm [81,82], obviously different from the emission peak of compound **2** (489 nm). Further, the free 2,2'-bipy ligand generally displays a weak luminescence at ca. 530 nm [83,84], also far from the emission peak of compound **3** (486 nm). The blue shifts of emission bands occurring in **2** and **3** are probably due to the cooperative effects of intraligand emission and ligand-to-metal charge transfer (LMCT) [42,85].

3.6. X-ray powder diffraction

In order to check the phase purity of these compounds, the X-ray powder diffraction (XRPD) of **1**, **2** and **3** were checked at room temperature. As shown in Figs. S11–S13, the peak positions of simulated and experimental XRPD patterns are in agreement with each other, indicating the good phase purity of these compounds. The differences in intensity may be due to the preferred orientation of the crystalline powder samples.

4. Conclusion

In summary, three new entangled Zn–ditetrazolate frameworks of **1–3** were hydrothermally synthesized by an in situ

ditetrazolate-ligand synthesis system assisted with various auxiliary N-donor ligands. These results demonstrate that the entangled Zn–ditetrazolate topological system can be modulated by choosing different secondary ligands. This work provides new paradigm for further rational design and synthesis of new entangled metal–organic frameworks via controlling auxiliary ligands. The blue emission of these compounds suggests that they may be potential candidates for blue-light emitting materials.

Supplementary materials

Crystallographic data for the structural analysis have been deposited with the Cambridge Crystallographic Data Center, CCDC reference numbers 695728, 695729 and 695730 for compounds 1–3, respectively. These data can be obtained free of charge at www.ccdc.cam.ac.uk/conts/retrieving.html (or from the Cambridge Crystallographic Data Centre, 12, Union Road, Cambridge CB2 1EZ, UK; fax: +44-1223/336-033; E-mail: deposit@ccdc.cam.ac.uk).

Acknowledgments

This work was supported by the National Natural Science Foundation of China (no. 20701005/20701006), the Post-doc station Foundation of Ministry of Education (no. 20060200002), the Analysis and Testing Foundation of Northeast Normal University and Science Foundation for Young Teachers of Northeast Normal University (no. 20070312/20070302).

Appendix A. Supplementary material

Supplementary data associated with this article can be found in the online version at [doi:10.1016/j.jssc.2008.12.022](https://doi.org/10.1016/j.jssc.2008.12.022).

References

- [1] L. Carlucci, G. Ciani, D.M. Proserpio, *Coord. Chem. Rev.* 246 (2003) 247–289.
- [2] O.R. Evans, W.B. Lin, *Acc. Chem. Res.* 35 (2002) 511–522.
- [3] S.R. Batten, K.S. Murray, *Coord. Chem. Rev.* 246 (2003) 103–130.
- [4] R.J. Hill, D.L. Long, N.R. Champness, P. Hubberstey, M. Schroder, *Acc. Chem. Res.* 38 (2005) 335–348.
- [5] M. Kawano, M. Fujita, *Coord. Chem. Rev.* 251 (2007) 2592–2605.
- [6] S. Kitagawa, R. Matsuda, *Coord. Chem. Rev.* 251 (2007) 2490–2509.
- [7] J.Y. Lu, *Coord. Chem. Rev.* 246 (2003) 327–347.
- [8] H. Chun, D.N. Dybtsev, H. Kim, K. Kim, *Chem. Eur. J.* 11 (2005) 3521–3529.
- [9] Y. Cui, S.J. Lee, W.B. Lin, *J. Am. Chem. Soc.* 125 (2003) 6014–6015.
- [10] B. Moulton, H. Abourahma, M.W. Bradner, J. Lu, G.J. McManus, M.J. Zaworotko, *Chem. Commun.* (2003) 1342–1343.
- [11] J.M. Lehn, *Science* 295 (2002) 2400–2403.
- [12] S.R. Batten, R. Robson, *Angew. Chem. Int. Ed.* 37 (1998) 1460–1494.
- [13] S. R Batten, *CrystEngComm*. 3 (2001) 67–72.
- [14] V.A. Blatov, L. Carlucci, G. Ciani, D.M. Proserpio, *CrystEngComm*. 6 (2004) 378–395.
- [15] X.H. Bu, M.L. Tong, H.C. Chang, S. Kitagawa, S.R. Batten, *Angew. Chem. Int. Ed.* 43 (2004) 192–195.
- [16] J.R. Li, Y. Tao, Q. Yu, X.H. Bu, H. Sakamoto, S. Kitagawa, *Chem. Eur. J.* 14 (2008) 2771–2776.
- [17] A. Withersby, A.J. Blake, N.R. Champness, P.A. Cooke, P. Hubberstey, M. Schroder, *J. Am. Chem. Soc.* 122 (2000) 4044–4046.
- [18] A. Galet, M.C. Munoz, J.A. Real, *J. Am. Chem. Soc.* 125 (2003) 14224–14225.
- [19] Q.M. Wang, G.C. Guo, T.C.W. Mak, *Chem. Commun.* (1999) 1849–1850.
- [20] L. Carlucci, G. Ciani, D.M. Proserpio, *Angew. Chem. Int. Ed.* 38 (1999) 3488–3492.
- [21] L. Carlucci, G. Ciani, F. Porta, D.M. Proserpio, L. Santagostini, *Angew. Chem. Int. Ed.* 41 (2002) 1907–1911.
- [22] L. Carlucci, G. Ciani, P. Macchi, D.M. Proserpio, S. Rizzato, *Chem. Eur. J.* 5 (1999) 237–243.
- [23] L. Carlucci, G. Ciani, D.M. Proserpio, S. Rizzato, *Chem. Eur. J.* 8 (2002) 1519–1526.
- [24] O.M. Yaghi, M. O’Keeffe, N.W. Ockwig, H.K. Chae, M. Eddaoudi, J. Kim, *Nature* 423 (2003) 705–714.
- [25] M. Eddaoudi, D.B. Moler, H.L. Li, B.L. Chen, T.M. Reineke, M. O’Keeffe, O.M. Yaghi, *Acc. Chem. Res.* 34 (2001) 319–330.
- [26] B.L. Chen, M. Eddaoudi, S.T. Hyde, M. O’Keeffe, O.M. Yaghi, *Science* 291 (2001) 1021–1023.
- [27] L.Y. Kong, Z.H. Zhang, H.F. Zhu, H. Kawaguchi, T. Okamura, M. Doi, Q. Chu, W.Y. Sun, N. Ueyama, *Angew. Chem. Int. Ed.* 44 (2005) 4352–4355.
- [28] H.F. Zhu, J. Fan, T. Okamura, Z.H. Zhang, G.X. Liu, K.B. Yu, W.Y. Sun, N. Ueyama, *Inorg. Chem.* 45 (2006) 3941–3948.
- [29] B. Moulton, M.J. Zaworotko, *Chem. Rev.* 101 (2001) 1629–1658.
- [30] R. Robson, *Dalton Trans.* (2008) 5113–5131.
- [31] B.J. Holliday, C.A. Mirkin, *Angew. Chem. Int. Ed.* 40 (2001) 2022–2043.
- [32] S. Leininger, B. Olenyuk, P.J. Stang, *Chem. Rev.* 100 (2000) 853–908.
- [33] M.W. Hosseini, *Acc. Chem. Res.* 38 (2005) 313–323.
- [34] P.J. Steel, *Acc. Chem. Res.* 38 (2005) 243–250.
- [35] L. Brammer, *Chem. Soc. Rev.* 33 (2004) 476–489.
- [36] S.R. Seidel, P.J. Stang, *Acc. Chem. Res.* 35 (2002) 972–983.
- [37] D.L. Caulder, K.N. Raymond, *Acc. Chem. Res.* 32 (1999) 975–982.
- [38] X.L. Wang, C. Qin, E.B. Wang, L. Xu, Z.M. Su, C.W. Hu, *Angew. Chem. Int. Ed.* 43 (2004) 5036–5040.
- [39] X.L. Wang, C. Qin, E.B. Wang, Y.G. Li, Z.M. Su, L. Xu, L. Carlucci, *Angew. Chem. Int. Ed.* 44 (2005) 5824–5827.
- [40] H.Q. Tan, Y.G. Li, Z.M. Zhang, C. Qin, X.L. Wang, E.B. Wang, Z.M. Su, *J. Am. Chem. Soc.* 129 (2007) 10066–10067.
- [41] X.L. Wang, C. Qin, E.B. Wang, Z.M. Su, Y.G. Li, L. Xu, *Angew. Chem. Int. Ed.* 45 (2006) 904–908.
- [42] X.L. Wang, C. Qin, E.B. Wang, Z.M. Su, *Chem. Eur. J.* 12 (2006) 2680–2691.
- [43] D.R. Xiao, E.B. Wang, H.Y. An, Z.M. Su, Y.G. Li, L. Gao, C.Y. Sun, L. Xu, *Chem. Eur. J.* 11 (2005) 6673–6686.
- [44] Y.G. Li, L.M. Dai, Y.H. Wang, X.L. Wang, E.B. Wang, Z.M. Su, L. Xu, *Chem. Commun.* (2007) 2593–2595.
- [45] C. Qin, X.L. Wang, L. Carlucci, M.L. Tong, E.B. Wang, C.W. Hu, L. Xu, *Chem. Commun.* (2004) 1876–1877.
- [46] X.L. Wang, C. Qin, E.B. Wang, Z.M. Su, L. Xu, S.R. Batten, *Chem. Commun.* (2005) 4789–4791.
- [47] X.L. Wang, C. Qin, E.B. Wang, Y.G. Li, Z.M. Su, *Chem. Commun.* (2005) 5450–5452.
- [48] X.L. Wang, C. Qin, E.B. Wang, Z.M. Su, *Chem. Commun.* (2007) 4245–4247.
- [49] Y.H. Wang, Y.W. Li, W.L. Chen, Y.G. Li, E.B. Wang, *J. Mol. Struct.* 877 (2008) 56–63.
- [50] Z.P. Demko, K.B. Sharpless, *J. Org. Chem.* 66 (2001) 7945–7950.
- [51] J.P. Zhang, X.M. Chen, *Chem. Commun.* (2006) 1689–1699.
- [52] X.M. Chen, M.L. Tong, *Acc. Chem. Res.* 40 (2007) 162–170.
- [53] X.M. Zhang, *Coord. Chem. Rev.* 249 (2005) 1201–1219.
- [54] H. Zhao, Z.R. Qu, H.Y. Ye, R.G. Xiong, *Chem. Soc. Rev.* 37 (2008) 84–100.
- [55] X.M. Zhang, M.L. Tong, X.M. Chen, *Angew. Chem. Int. Ed.* 41 (2002) 1029–1031.
- [56] S. Hu, J.C. Chen, M.L. Tong, B. Wang, Y.X. Yan, S.R. Batten, *Angew. Chem. Int. Ed.* 44 (2005) 5471–5475.
- [57] R.G. Xiong, X. Xue, H. Zhao, X.Z. You, B.F. Abrahams, Z.L. Xue, *Angew. Chem. Int. Ed.* 41 (2002) 3800–3803.
- [58] X. Xue, X.S. Wang, L.Z. Wang, R.G. Xiong, B.F. Abrahams, X.Z. You, Z.L. Xue, C.M. Che, *Inorg. Chem.* 41 (2002) 6544–6546.
- [59] Z.R. Qu, H. Zhao, X.S. Wang, Y.H. Li, Y.M. Song, Y.J. Liu, Q. Ye, R.G. Xiong, B.F. Abrahams, Z.L. Xue, X.Z. You, *Inorg. Chem.* 42 (2003) 7710–7712.
- [60] Q. Ye, Y.H. Li, Y.M. Song, X.F. Huang, R.G. Xiong, Z.L. Xue, *Inorg. Chem.* 44 (2005) 3618–3625.
- [61] X.S. Weng, Y.Z. Tang, X.F. Huang, Z.R. Qu, C.M. Che, P.W.H. Chan, R.G. Xiong, *Inorg. Chem.* 44 (2005) 5278–5285.
- [62] J.Y. Zhang, A.L. Cheng, Q. Yue, W.W. Sun, E.Q. Gao, *Chem. Commun.* (2008) 847–849.
- [63] T. Wu, B.H. Yi, D. Li, *Inorg. Chem.* 44 (2005) 4130–4132.
- [64] J.R. Li, Y. Tao, Q. Yu, X.H. Bu, *Chem. Commun.* (2007) 1527–1529.
- [65] J. Tao, Z.J. Ma, R.B. Huang, L.S. Zheng, *Inorg. Chem.* 43 (2004) 6133–6135.
- [66] L.Z. Wang, X.S. Wang, Y.H. Li, Z.P. Bai, R.G. Xiong, M. Xiong, G.W. Li, *Chin. J. Inorg. Chem.* 18 (2002) 1191–1194.
- [67] H. Zhao, Q. Ye, Q. Wu, Y.M. Song, Y.J. Liu, R.G. Xiong, *Z. Anorg. Allg. Chem.* 630 (2004) 1367–1370.
- [68] Y.C. Wang, H. Zhao, Y.M. Song, X.S. Wang, R.G. Xiong, *Appl. Organomet. Chem.* 18 (2004) 494–495.
- [69] X.H. Huang, T.L. Sheng, S.C. Xiang, R.B. Fu, S.M. Hu, Y.M. Li, X.T. Wu, *Chin. J. Struct. Chem.* (2007) 161–164.
- [70] M. Dincă, A.F. Yu, J.R. Long, *J. Am. Chem. Soc.* 128 (2006) 8904–8913.
- [71] G.M. Sheldrick, SHELXL97, Program for Crystal Structure Refinement, University of Göttingen, Göttingen, Germany, 1997.
- [72] G.M. Sheldrick, SHELXS97, Program for Crystal Structure Solution, University of Göttingen, Göttingen, Germany, 1997.
- [73] V.A. Blatov, TOPOS, A multipurpose Crystallochemical Analysis with the Program Package, Samara State University, Russia, 2004.
- [74] C. Janiak, *J. Chem. Soc. Dalton Trans.* (2000) 3885–3896.
- [75] L. Carlucci, G. Ciani, D.M. Proserpio, S. Rizzato, *CrystEngComm*. 4 (2002) 121–129.
- [76] Y.H. Wang, B. Bredenkötter, B. Riegera, D. Volkmer, *Dalton Trans.* (2007) 689–696.
- [77] X. He, C.Z. Lu, Y.Q. Yu, S.M. Chen, X.Y. Wu, Y. Yan, *Z. Anorg. Allg. Chem.* 630 (2004) 1131–1135.

- [78] X.Y. Wang, L. Wang, Z.M. Wang, S. Gao, *J. Am. Chem. Soc.* 128 (2006) 674–675.
- [79] T.F. Liu, D. Fu, S. Gao, Y.Z. Zhang, H.L. Sun, G. Su, Y.J. Liu, *J. Am. Chem. Soc.* 125 (2003) 13976–13977.
- [80] Y.Z. Zhang, H.Y. Wei, F. Pan, Z.M. Wang, Z.D. Chen, S. Gao, *Angew. Chem. Int. Ed.* 44 (2005) 5841–5846.
- [81] X.Q. Wang, J.K. Cheng, Y.H. Wen, J. Zhang, Z.J. Li, Y.G. Yao, *Inorg. Chem. Commun.* 8 (2005) 897–899.
- [82] P.X. Yin, J. Zhang, J.K. Cheng, Z.J. Li, Y.G. Yao, *Inorg. Chem. Commun.* 9 (2006) 541–543.
- [83] J. Tao, J.X. Shi, M.L. Tong, X.X. Zhang, X.M. Chen, *Inorg. Chem.* 40 (2001) 6328–6330.
- [84] J. Zhang, Y.C. Shen, Y.Y. Qin, Z.J. Li, Y.G. Yao, *CrystEngComm* 9 (2007) 636–639.
- [85] K. Balasubramanian, *Relativistic Effects in Chemistry. Part A: Theory and Techniques; Part B: Applications*, Wiley, New York, 1997.